Sensor and Simulation Notes

Note 429

September 1998

Design and Optimization of a Conical Transmission-Line Feed for a Coaxial Beam-Rotating Antenna

Clifton C. Courtney and David Slemp
Voss Scientific
Albuquerque, NM

Carl E. Baum and Robert Torres
Air Force Research Laboratory / Directed Energy Directorate
Albuquerque, NM

ABSTRACT

In this note several considerations for the design of the COBRA III antenna are presented. The COBRA III prototype antenna uses a Cassegrain-type configuration with a paraboloidal main reflector and a hyperboloidal subreflector. The feed structure will be a conical coaxial transmission line that has its vertex at the vertex of the paraboloidal reflector, and whose center conductor which will attach directly to the subreflector. This note presents two methods (related) to find the optimum subreflector size as a function of the transmission feed line electric field mode and main reflector size. The method is general, meaning the optimum subreflector size can be found for any feed aperture distribution. Here we approximate the aperture feed distribution to be that of a truncated coaxial transmission line. The dimensions of the optimum subreflector for the COBRA III prototype are then computed which result in a subreflector size (for a fixed main reflector diameter) that results in the peak gain achievable. Additionally, the main and subreflector dimensions specify the dimensions of the conical transmission feed line. The dimensions of the conical transmission feed line are computed, and the match to a 50Ω feed system is discussed. Also, since an important application of the COBRA design will be as an antenna for high power microwave sources, a calculation of the optimum coaxial transmission line impedance is presented. This optimum value will minimize the peak electric field for a given power level. It will be shown that the system impedance associated with a peak gain configuration is different from the system impedance associated with the configuration to minimize the electric field in the feed line. Thus, the system impedance can be bounded by the impedances of the peak gain and minimum field conditions. Finally, a summary of the complete COBRA III prototype design is given.

Table of Contents

Acknowledgement - This work was sponsored by the United States Air Force under a Small Business Innovation for Research Phase II program, contract no. F29601-97-C-0005.

1. INTRODUCTION

In this note several considerations for the design of the Coaxial Beam-Rotating Antenna (COBRA) III are presented. The COBRA III prototype antenna is the third in a line of prototype antennas that use structural modifications of reflecting surfaces to modify the aperture distribution of an azimuthally symmetric distribution to realize a boresight peak with circular polarization. Whereas the previous prototype antennas used circular aperture feed horns to illuminate the main reflector, the COBRA III prototype antenna will use the center conductor of a conical transmission line to drive a hyperboloidal subreflector. The field that is propagated along the transmission line feed will strike the subreflector, be reflected, and in turn will illuminate the main reflector. As was the case with the previous prototypes, the main reflector has been divided into 4 equal segments, and these segments are adjusted in the usual way [1, 2] to produce a boresight peak with circular polarization. A schematic diagram of the COBRA III is shown in Figure 1.

As indicated in the figure the antenna feed will be a conical transmission line with its vertex at the vertex of the paraboloidal reflector. The conical transmission line will have a nominal characteristic impedance of Z_0 based on the half angles of the inner and outer conductors of the transmission line. The inner conductor will attach to the directly to the subreflector and have a nominal diameter that extends across the subreflector's shadow boundary. The outer conductor will continue from the vertex, to a point along the conical path just before it intercepts the inner most ray path off of the subreflector. At this point the edge will be turned and radiused, and it will continue along a path parallel with the innermost ray path. It will not terminate on the main reflector, rather it will stop abruptly at a point where it will clear all of the moving surfaces of the main reflector.

The design of the conical transmission line feed system for the COBRA III has led to consideration of the question: What is the optimum size subreflector for a given main reflector size? The trade off is between the desire to maximize the physical aperture size, and to illuminate the available aperture area is such a way that produces a maximum boresight gain. This optimization is needed because the electric field distribution in the aperture is not constant, in fact it is a maximum at the interior and falls off (at a rate dictated by the transmission line mode) at the outer extremes of the annular aperture formed by the main reflector and the subreflector. The topics of this note are as follows. First, the assumptions made concerning the propagation of the microwave power from the transmission line, to the subreflector and into the main reflector will be stated. Next, an outline of two related analysis and optimization methods will be given. The results of the analysis will then be presented, and an optimum subreflector diameter determined. The diameters of the main reflector and the subreflector will then be used to design the conical transmission line feed.

In addition, considering the possible use of the COBRA designs with high power microwave (HPM) sources [3, 4] a calculation of the optimum coaxial transmission line

impedance is presented. This optimum value will minimize the peak electric field for a given power level. It will be shown that the system impedance associated with a peak gain configuration is different from the system impedance associated with the configuration to minimize the electric field in the feed line. Thus, the system impedance can be bounded by the impedances of the peak gain and minimum field conditions. Finally, an overview of the design of the COBRA III antenna is presented.

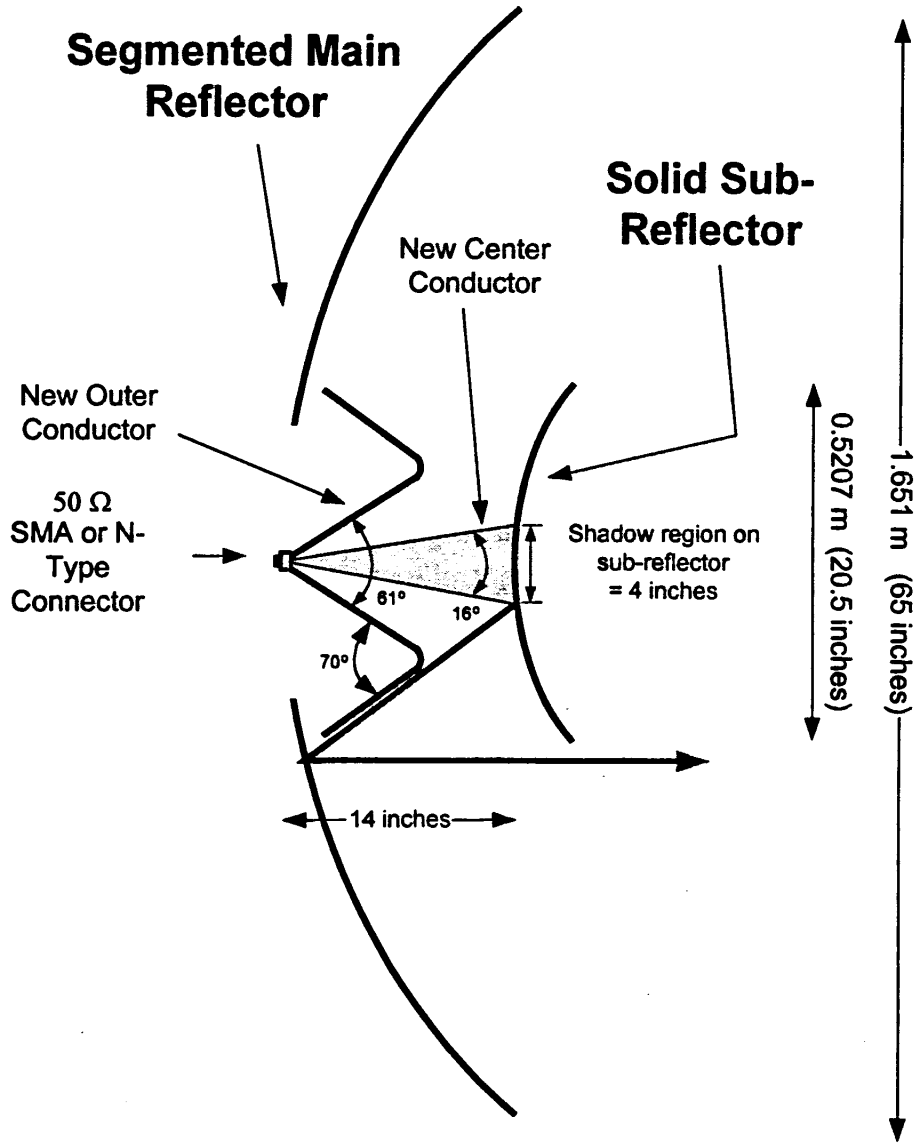

Figure 1. A schematic diagram of the COBRA III prototype design.

2. ANALYSIS ASSUMPTIONS

To permit a straightforward analysis of the radiating properties of the COBRA III, certain problem simplifications and assumptions were used to reduce the complexity and permit an optimization of the subreflector diameter. The problem simplifications are:

1. The field distribution in the aperture of the conical transmission, at the cross sectional position where the center conductor leaves the outer conductor, is assumed to be that of the TEM mode in a coaxial cable with equivalent inner and outer diameters.

2. All of the power in the aperture is delivered from the transmission line aperture to the subreflector, there is no reflection of the power due to a transmission line impedance mismatch.

3. The field propagates to the subreflector, and is scattered into the main reflector in an optical-like manner.

4. The field distribution in the main aperture has the same characteristic (distribution) as the field distribution in the assumed coaxial aperture. This assumption becomes exact in the high frequency limit. The value of the electric field is adjusted so that total power is conserved through the system.

These simplifying assumptions will permit the development of a simple method to compute the radiated boresight field as a function of the subreflector size.

3. ANALYSIS TECHNIQUES

In this section the analysis method is outlined. This includes the computation of the transmission line power, the projection and scaling of the electric field from the coaxial aperture into the main annular aperture, the computation of the boresight radiated field, and the optimization procedures to compute the ratio of the subreflector to main reflector diameter to yield maximum gain.

3.1 Available Power in the Coaxial Aperture

If the TEM coaxial mode is assumed to be propagating in a coaxial cable with inner and outer radii of r_a and r_b respectively, then the electric field distribution is given by

$$\mathbf{E} = \hat{\rho} \frac{V_{ab}}{\ln(r_b / r_a)} \frac{1}{\rho} \tag{1}$$

where V_{ab} = transmission line voltage and is the potential difference between the inner and outer conductors. The power in the coaxial aperture is

$$Power = \int_0^{2\pi} \int_{r_a}^{r_b} (\mathbf{E} \times \mathbf{H}^*) \cdot \hat{\mathbf{z}} \, \rho \, d\rho \, d\phi = \int_0^{2\pi} \int_{r_a}^{r_b} \frac{|\mathbf{E}|^2}{\eta_0} \rho \, d\rho \, d\phi = \frac{2\pi}{\eta_0} \frac{V_{ab}^2}{\ln(r_b / r_a)} \tag{2}$$

for a circular coaxial aperture with its axis aligned along the z-axis and where $\eta_0 = \sqrt{\mu_0 / \varepsilon_0}$. This can also be written as

$$Power = V_{ab}^2 / Z_0 \tag{3}$$

where $Z_0 = \frac{\eta_0}{2\pi} \ln(r_b / r_a)$ is the characteristic impedance of the coaxial cable.

3.2 *Electric Field Projection and Scaling*

As the electric field is guided from the aperture by the center conductor of the coaxial cable to the subreflector and is scattered into the main reflector, it is assumed that the field distribution spreads in such a way that power is preserved. A simple depiction of this projection, or spreading, is shown in Figure 2.

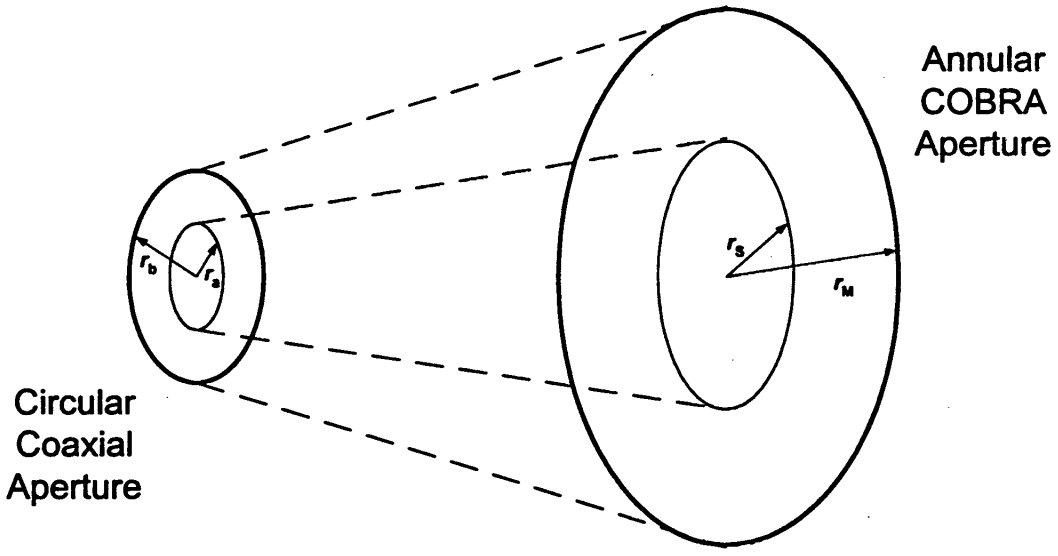

Figure 2. The electric field of the circular coaxial aperture is projected onto the annular aperture of the COBRA (defined by the diameters of the main reflector and the subreflector).

To have equal power in both apertures, the following relation must hold

$$\frac{2\pi}{\eta_0}\frac{V_{ab}^2}{\ln(r_b/r_a)} = \frac{2\pi}{\eta_0}\frac{V_{SM}^2}{\ln(r_M/r_S)} \tag{4}$$

where r_M and r_S are the radii of the main reflector and the subreflector respectively, and V_{SM} = the equivalent voltage. The relationship between the coaxial line voltage and the equivalent voltage is easily found to be

$$V_{SM} = V_{ab}\sqrt{\frac{\ln(r_M/r_S)}{\ln(r_b/r_a)}} \tag{5}$$

which is then used to define a new electric field distribution in the aperture in terms of the coaxial line voltage

$$\mathbf{E}_{aperture} = \hat{\varrho}\,\frac{V_{SM}}{\ln(r_M/r_S)}\frac{1}{\rho} = \hat{\varrho}\,\frac{V_{ab}}{\ln(r_M/r_S)}\sqrt{\frac{\ln(r_M/r_S)}{\ln(r_b/r_a)}}\frac{1}{\rho}. \tag{6}$$

3.3 *Aperture Field Modification by the Segmented Main Reflector*

To this point the assumptions have been that the transmission line traveling wave leaves the circular coaxial aperture without reflection, and travels to the subreflector confined within the volume that would be bounded by the inner conductor of the concial transmission line and the outer conductor – had it extended onward to terminate on the outer periphery of the subreflector. Furthermore, we have assumed that the field is scattered from the subreflector into the main reflector and again spreads just to the point that it fills the main reflector with a distribution that is like the field distribution in the circular coaxial aperture of the transmission line.

The COBRA achieves its unique properties by adjusting path lengths from the focal point of the main reflector to the antenna aperture in a prescribed manner [5]. This path length adjustment is equivalent to adding a phase shift ($\Psi(\phi)$) to the portion of the electric field illumination that is a function of the azimuthal coordinate. For a main reflector with a surface that has been partitioned into four equal segments the amount of the phase shift is given by

$$\Psi(\phi) = \begin{cases} 0, & 0 \le \phi < \pi/2 \\ \pi/2, & \pi/2 \le \phi < \pi \\ \pi, & \pi \le \phi < 3\pi/2 \\ 3\pi/2, & 3\pi/2 \le \phi < 2\pi \end{cases} \tag{7}$$

The field then travels from the surface of the main reflector to the aperture in a collimated fashion without spreading, and with the phase shift indicated above. Then, the field distribution in the antenna aperture is

$$\mathbf{E}_{aperture}(\rho,\phi) = \hat{\varrho}\,\frac{V_{ab}}{\ln(r_M/r_S)}\sqrt{\frac{\ln(r_M/r_S)}{\ln(r_b/r_a)}}\,\frac{1}{\rho}\,e^{j\Psi(\phi)}, \qquad r_S \le \rho \le r_M . \tag{8}$$

3.4 Computation of Radiated Field and Subreflector Size Optimization

The radiated field is computed directly in the usual way from knowledge of the aperture field distribution (Eq. 9). According to [6] the radiated field can be written as

$$\mathbf{E}_{radiated}(r,\theta,\phi) = j k_0 \frac{\cos\theta}{2\pi}\frac{e^{-jk_0 r}}{r}\mathbf{f}(k_x,k_y) \tag{9}$$

where $k_x = k_0 \sin\theta\cos\phi$ and $k_y = k_0 \sin\theta \sin\phi$, and $k_0 = 2\pi/\lambda$. The term $\mathbf{f}(k_x,k_y)$ is actually the 2-dimensional Fourier transform of the aperture field and in carteesian coordinates is given by

$$f_x(k_x,k_y) = \iint_{S_A} \mathbf{E}_A(\mathbf{r}')\cdot\hat{\mathbf{a}}_x\, e^{j(k_x x + k_y y)}\, dA' \tag{10a}$$

$$f_y(k_x,k_y) = \iint_{S_A} \mathbf{E}_A(\mathbf{r}')\cdot\hat{\mathbf{a}}_y\, e^{j(k_x x + k_y y)}\, dA' \tag{10b}$$

where $\mathbf{E}_A(\mathbf{r}')$ is the aperture electric field distribution. For an aperture with circular boundaries

$$f_{(x,y)}(k_x,k_y) = \int_0^{2\pi}\int_{r_S}^{r_M} \mathbf{E}_A(\mathbf{r}')\cdot\hat{\mathbf{a}}_{(x,y)}\, e^{jk_0\rho'\sin\theta\cos(\phi-\phi')}\,\rho'\,d\rho'\,d\phi' \tag{11}$$

Finally, the far-zone electric field in spherical coordinates is

$$\mathbf{E}_{radiated}(r,\theta,\phi) = jk_0 \frac{e^{-jk_0 r}}{2\pi r}\left[\hat{\mathbf{a}}_\theta (f_x \cos\phi + f_y \sin\phi) + \hat{\mathbf{a}}_\theta \cos\theta (f_y \cos\phi - f_x \sin\phi)\right] \quad (12)$$

The optimum value of the subreflector size is defined as the value of subreflector radius r_S that maximizes the boresight electric field. Assuming an aperture field distribution (Eqn. 8) the optimum subreflector diameter is then determined by computing the radiated field (Eqns. 12) for all practical values of subreflector radius $0 < r_S < r_M$.

3.5 *Alternate Analysis and Optimization Technique*

Another, more direct, approach to the problem can be formulated. From [1] the boresight radiated electric vector potential of a COBRA aperture is given by

$$F_x(r,\theta,\phi) = \frac{e^{jk_0 r}}{2\pi r} \sum_{n=1}^{N} \int_{\phi_{n-1}}^{\phi_n} \int_{r_S}^{r_M} E_\rho(\rho') \sin(\phi')\, \rho' d\rho' d\phi' \quad (13)$$

where $E_\rho(\rho)$ = the azimuthally symmetric electric field in the aperture, and $\phi_n = \frac{2\pi}{N}(n-1)$ for an aperture created with N equal segments (either in the main reflector or the subreflector. This can be factored and re-written as

$$F_x(r,\theta,\phi) = \frac{e^{jk_0 r}}{2\pi r} \underbrace{\left[2\pi \int_{r_S}^{r_M} E_\rho(\rho')\, \rho' d\rho'\right]}_{\Theta(\rho)} \underbrace{\left[\frac{1}{2\pi} \sum_{n=1}^{N} e^{j\frac{2\pi(n-1)}{N}} \left[\cos\phi_{n-1} - \cos\phi_n\right]\right]}_{\xi_x(N)} \quad (14)$$

The term $\zeta_x(N)$ is independent of the inner and outer radii, so the procedure can concentrate on the optimization of the $\Theta(\rho)$ term. To do so, one must first assume an electric field aperture distribution. In this case we assume a distribution of the form

$$E_\rho(\rho) = \frac{\gamma}{\rho} \quad (15)$$

where $\gamma = \frac{V_{ab}}{\ln(r_M / r_S)} \sqrt{\frac{\ln(r_M / r_S)}{\ln(r_b / r_a)}}$ and is a constant of proportionality that maintains conservation of power in the aperture. Then

$$\Theta(\rho) = 2\pi \int_{r_S}^{r_M} E_\rho(\rho')\, \rho' d\rho' = 2\pi\alpha \int_{r_S}^{r_M} \frac{1}{\rho}\, \rho' d\rho' = 2\pi\gamma (r_M - r_S) \quad (16)$$

and it is desired to optimize this value subject to the value of the inner radius r_S. Some simple algebraic manipulations yield the following

$$\Theta(\rho) = 2\pi \frac{V_{ab}}{\sqrt{\ln(r_b / r_a)}} \frac{(r_M - r_S)}{\sqrt{\ln(r_M / r_S)}} \tag{17}$$

so that it is sufficient to maximize the term $\frac{(r_M - r_S)}{\sqrt{\ln(r_M / r_S)}}$, or equivalently to maximize the function

$$f(r_S) = \frac{(r_M - r_S)^2}{\ln(r_M / r_S)} = (r_M)^2 \frac{(1 - r_S / r_M)^2}{\ln(r_M / r_S)} = (r_M)^2 \frac{(1-\alpha)^2}{\ln(1/\alpha)} = -(r_M)^2 \frac{(1-\alpha)^2}{\ln(\alpha)} \tag{18}$$

where $\alpha = r_S / r_M$. The size of the radius of the subreflector is bounded by $0 \le r_S \le r_M$, or $0 \le \alpha \le 1$.

4. ANALYSES RESULTS

The optimization of the subreflector diameter was conducted using each of the two methods described. These results are presented here.

4.1 Results of the First Method

The radiated field and boresight gain was computed for the possible range of values that the diameter of the subreflector could take. In other words, for

$$0 < r_S < r_M = 32.5 \text{ inches} \tag{19}$$

where r_S = radius of the subreflector and r_M = radius of the main reflector. In Table 1 is presented the physical aperture gain and the computed boresight gain for circular polarization for a number of values of subreflector diameter values. The aperture of the antenna is assumed to lie in the xy-plane, then the boresight direction is $(\theta = 0^o, \phi = 0^o)$. The physical aperture gain is simply

$$G_A = 10 Log\left[\frac{4\pi}{\lambda^2} Area\right] = 10 Log\left[\left(\frac{2\pi}{\lambda}\right)^2 \left(r_M^2 - r_S^2\right)\right] \tag{20}$$

The circular boresight gain is determined by computing the gain of a single linear component of the radiated field on boresight, and adding 3-dB to it [1].

The trend in the results is clear at either extreme ($r_S \to 0$ or $r_S \to r_M$) of possible values for the subreflector diameter, the gain falls off. At these extreme values the computed boresight gain is extremely sensitive to the value of the subreflector diameter. At intermediate values $r_S \approx r_M / 2$ the boresight gain is about optimum, and is a weak function of the subreflector diameter. For the values computed it seems the optimum value for the subreflector diameter is about 19 inches:

$$\text{optimum } r_S = 9.5 \text{ inches} \tag{21}$$

Graphs of the data presented in Table 1 are shown in Figure 3. In Figure 3a the data is plotted against a logarithmic abscissa, while in Figure 3b the data is plotted against a linear abscissa. Both representations clearly show the trends and result described above. The subreflector diameter size of the COBRA III was chosen to be 20.5 inches, since this will allow us to utilize an existing piece of hardware without sacrificing performance (see the data in the table below).

Table 1. **The physical aperture gain and the computed boresight gain for circular polarization are presented for a number of values of subreflector diameter values.**

Subreflector Size inches	Aperture Gain dB	Cir-Pol Boresight Gain dB
1	34.1681	26.9202
3	34.1596	27.9722
5	34.1426	28.4758
10	34.0618	29.0846
15	33.9238	29.3108
20	33.7229	29.3359
20.5	**33.6991**	**29.3298**
25	33.4501	29.2132
30	33.0917	28.9579
35	32.6259	28.5641
40	32.0180	28.0064
45	31.2074	27.2301
50	30.0759	26.1212
55	28.3435	24.4025
60	25.0004	21.0662
63	19.0836	15.1508

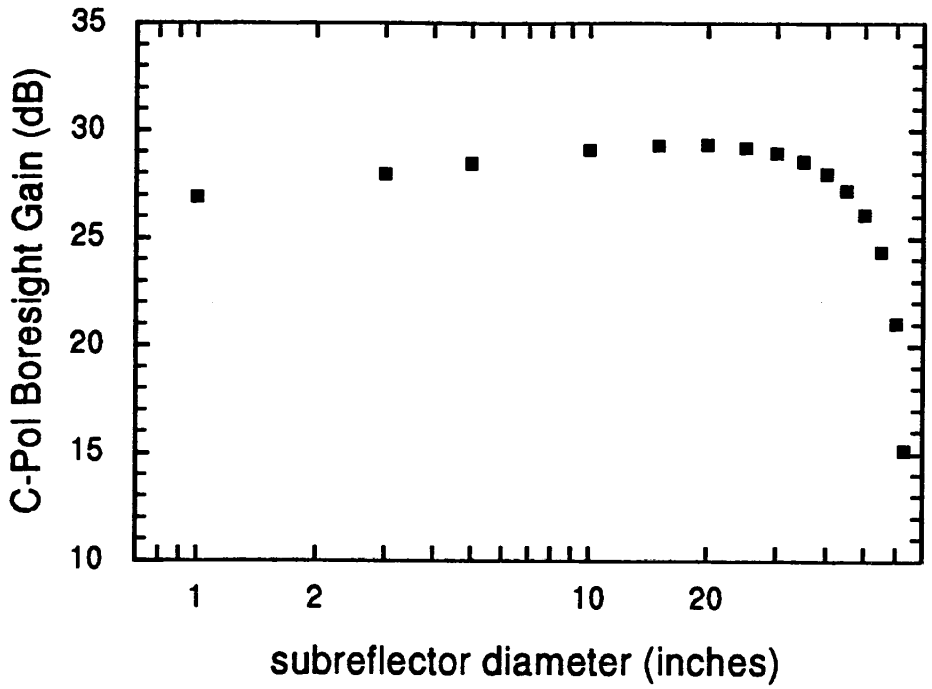

(a)

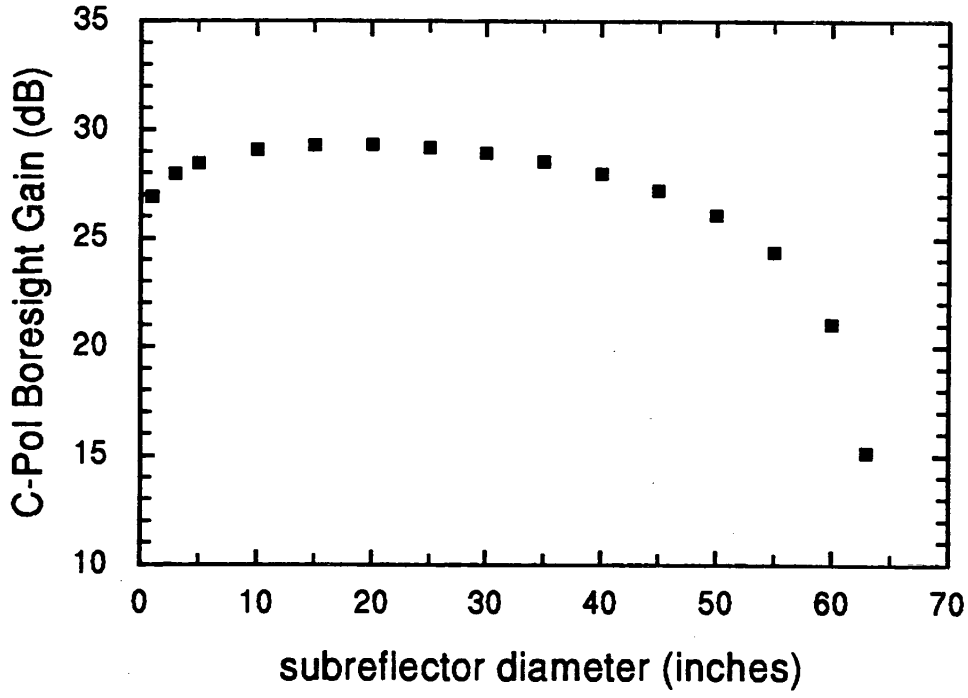

(b)

Figure 3. **Circularly-Polarized boresight gain as a function of the subreflector diameter: (a) logarithmic abscissa axis; and (b) linear abscissa axis.**

4.2 *Results of the Second Method*

To maximize the expression of Eq. 18, simply differentiate with respect to r_S, set the result to 0, then solve for r_S.

$$\frac{d}{d\alpha} f(\alpha) = -(r_M)^2 \frac{d}{d\alpha}\left\{\frac{(1-\alpha)^2}{\ln(\alpha)}\right\} = 0 \tag{22}$$

or,

$$\frac{d}{d\alpha}\left\{\frac{(1-\alpha)^2}{\ln(\alpha)}\right\} = \frac{2(1-\alpha)(-1)}{\ln(\alpha)} + (-1)\frac{(1-\alpha)^2}{(\ln(\alpha))^2}\frac{1}{\alpha} = 0 \tag{23}$$

and simplifying

$$(1-\alpha) + 2\alpha\ln(\alpha) = 0 \tag{24}$$

to obtain the function we wish to solve. Unfortunately Eq. 24 is difficult to solve analytically. However, if we plot Eq. 24 over the interval $0 \le \alpha \le 1$ (all possible physical values of the ratio of the subreflector to the main reflector) then the result shown in Figure 4 is obtained.

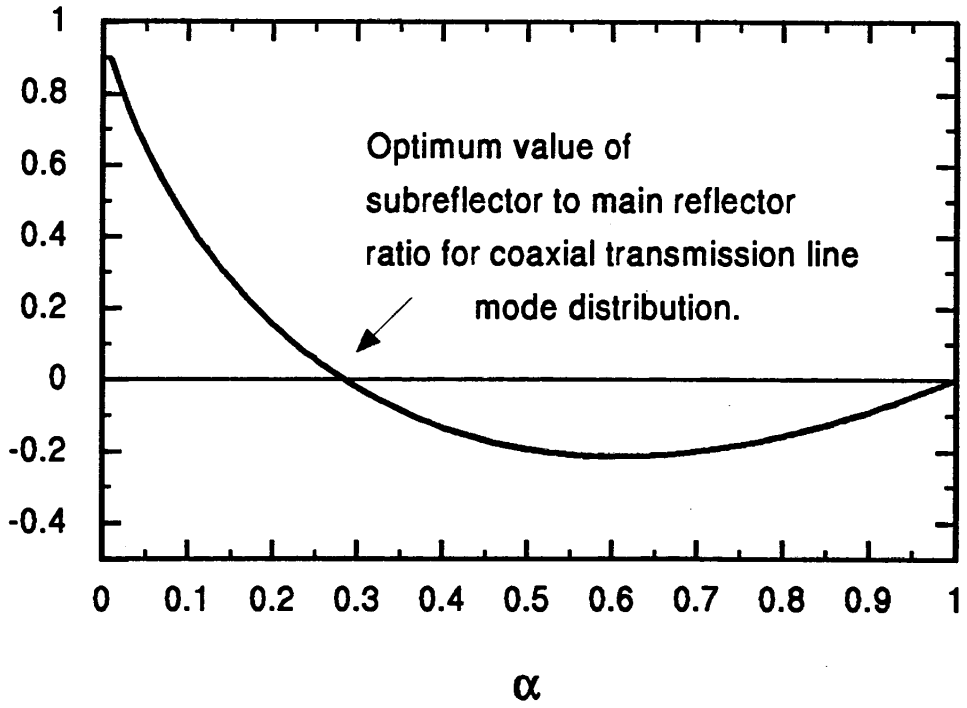

Figure 4. **The optimizing function, Eq. 24, is plotted over the possible values of the ratio of the subreflector radius to the main reflector radius.**

Using a root finding method it can be shown that the function, Eq. 24, has a zero at $\alpha = 0.284668$, which then yields a value for the optimum reflector size of

$$\text{optimum } r_S = r_M \times \alpha = 9.2517 \text{ inches} \tag{25}$$

which is very close to the value obtained using the previous method.

Since these two methods are logically equivalent (they both are based on the computation of the boresight field) it is not surprising that the same optimum value is found. Both methods were presented since each gives a slightly different perspective on the problem.

4.3 Optimum Coaxial Transmission Line Impedance

A principal application of COBRA-type antennas will be their use with High Power Microwave (HPM) sources that produce microwave output power in azimuthally symmetric modes [3, 4, 7]. Of particular concern in many HPM sources is the reduction of the peak electric field. Electric field breakdown is known to cause deterioration of the performance (reduced output power and energy, pulse shortening, etc.) of HPM sources [8]. Consequently an antenna design and feed method that minimizes the peak electric field would be of interest. A method similar to that used above can be used to determine the coaxial transmission line impedance that, for a given power level and outer conductor diameter, minimizes the peak electric field.

The electric field distribution in coaxial geometry is given in (Eqn. 1), and it is clear that the peak value occurs at the surface of the inner conductor

$$E_{peak} = \left| \mathbf{E}(\rho = r_a) \right| = \frac{V_{ab}}{\ln(r_b / r_a)} \frac{1}{r_a} \tag{26}$$

The power delivered in a coaxial line is

$$Power = P = \frac{2\pi}{\eta_0} \frac{V_{ab}^2}{\ln(r_b / r_a)} = \frac{2\pi}{\eta_0} \frac{1}{\ln(r_b / r_a)} \left[E_{peak} \ln(r_b / r_a) r_a \right]^2, \tag{27}$$

or the peak field in terms of a constant power is

$$E_{peak} = \frac{1}{r_a} \sqrt{\frac{\eta_0}{2\pi} \frac{P}{\ln(r_b / r_a)}}. \tag{28}$$

To find the optimum coaxial impedance, differentiate the above and solve for the zero of

$$\frac{dE_{peak}}{d(r_a)} = \frac{d}{d(r_a)}\left\{\frac{1}{r_a}\sqrt{\frac{\eta_0}{2\pi}\frac{P}{\ln(r_b/r_a)}}\right\} = 0, \tag{29}$$

which is equivalent to solving

$$1 - 2\ln(1/r_a) = 0. \tag{30}$$

The value of r_a that solves this expression is found to be $r_a = e^{-\frac{1}{2}} \approx 0.606531$, and the resulting optimal value for the coaxial impedance that minimizes the peak electric field for a constant power is

$$Z_C = \frac{\eta_0}{2\pi}\ln(r_b/r_a) = \frac{\eta_0}{2\pi}\ln(e^{\frac{1}{2}}) = 30\Omega \tag{31}$$

This value for the coaxial impedance minimizes the peak electric field in the transmission line for a given amount of delivered microwave power.

4.4 System Impedance

The system impedance for the COBRA III is defined as the coaxial transmission line impedance that would result when the diameter of the inner conductor equals that of the subreflector, and the diameter of the outer conductor equals that of the main reflector. Then,

$$Z_{System} = \frac{\eta_0}{2\pi}\ln(r_b/r_a) \tag{32}$$

The system impedance found to be optimum if one wishes to maximize the boresight gain is then

$$Z_{System}^{Peak\ Gain} = \frac{\eta_0}{2\pi}\ln(r_b/r_a) = \frac{377}{2\pi}\ln(1/0.284668) = 75.4\Omega \tag{33}$$

The system impedance found to be optimum if one wishes to minimize the peak electric field in the feed and antenna component of the system is then

$$Z_{System}^{Minimum\ Field} = \frac{\eta_0}{2\pi}\ln(r_b/r_a) = \frac{377}{2\pi}\ln(e^{\frac{1}{2}}) = 30\Omega \tag{34}$$

The system impedance for the COBRA III antenna is then bounded by

$$Z_{System}^{Minimum\ Field} = 30\Omega \le Z_{System} \le Z_{System}^{Peak\ Gain} = 75\Omega. \tag{35}$$

5. CONICAL TRANSMISSION LINE DESIGN

In the COBRA III prototype design we are driven more by the desire to demonstrate the antenna concepts and realize the peak boresight gain, than we are in minimizing the peak electric field. The source and antenna measurements will be conducted with low power, therefore the optimal value of the radius of the subreflector is determined by the peak gain consideration. The design and geometry of the feed will be subject to three restrictions:

1. The diameter of the inner conductor will be equal to the shadow area of the subreflector;
2. The diameter of the outer conductor would be equal to the diameter of the subreflector, should it extend to the outer conductor; and
3. The outer conductor of the transmission line will extend outward just to the point where it intercepts the ray from the subreflector.

These constraints result in the shape of the feed structure being as shown in Figure 1. This section uses the results of the earlier analysis to quantify the design and dimensions of the conical transmission line feed.

As it turns out, it has been shown that the paraboloidal reflector exactly transforms a spherical TEM wave (such as that supported by the conical coaxial transmission line) into a planar TEM wave [9]. Then it is reasonable to expect that once the value of the system gain has been determined, the impedance of the conical feed transmission line is determined to be that which matches the system impedance defined by the diameters of the main and subreflectors. It will be shown that this is the case, and is compatible with the above criteria.

5.1 Characteristic Impedance of a Conical Transmission Line

The characteristic impedance of a conical transmission line is given by

$$Z_0 = \frac{377}{2\pi} \ln\left[\frac{\cot(\theta_1/2)}{\cot(\theta_2/2)}\right] \tag{36}$$

[10] for a free space dielectric. The angles correspond to the inner and outer half angles of the conical conductors, as shown in Figure 5.

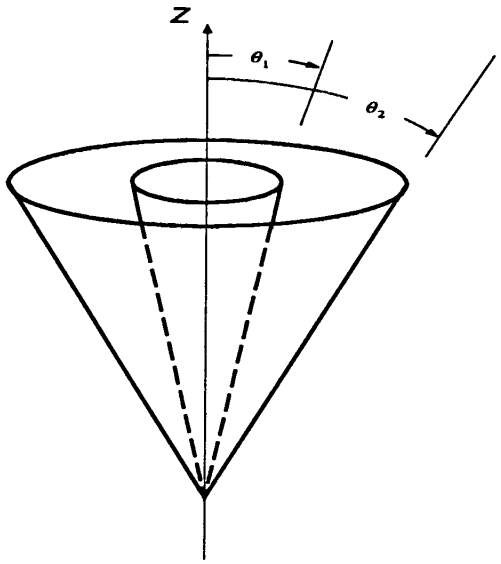

Figure 5. The geometry of a conical transmission line.

5.2 Design of the Conical Transmission Line Feed

The dimensions of the conical transmission line feed are dictated by the need to optimally illuminate the main reflector. The earlier analysis has given the optimum value of the radius of the subreflector. Next, we specify that the conjugate focus of the subreflector is at the vertex of the main reflector. This implies that the vertex of the conical transmission line be located there as well so that the wave incident on the subreflector will be spherical with its origin in the proper place – the conjugate focus of the subreflector. Other considerations are that the diameter of the inner conductor, as it terminates on the subreflector, should be equal to the diameter of the shadow region of the subreflector. The half-angle of the outer conductor should be such that the outer conductor would extend to the edge of the subreflector, should it continue that far. These considerations and restrictions completely define the geometry of the conical transmission line feed.

The required conical transmission line feed needed for the third COBRA prototype antenna will have the following dimensions. The radius of the subreflector is slightly oversized at $r_S = 10.25$ inches, the distance of the front face of the subreflector to the vertex of the main reflector is approximately 14, and the diameter of the subreflector shadow region is about 4 inches. This defines the half-angle of the inner conductor to be

$$\theta_1 = \tan^{-1}\left(\frac{4/2}{14}\right) = 8.13^{o}. \tag{37}$$

The half-angle of the outer conductor is defined by the flare angle needed to insure that the outer conductor would cover the subreflector, should it extend to that point. Then, the diameter of the outer conductor would be 20.5 inches, and the length will be the sum of the distance from the vertex of the main reflector to the front face of the subreflector and the thickness of the subreflector – which is 3.5 inches. This defines the half-angle of the outer conductor to be

$$\theta_2 = \tan^{-1}\left(\frac{20.5/2}{14+3.5}\right) = 30.35^o . \tag{38}$$

The resulting impedance of the conical transmission line is then

$$Z_0 = \frac{377}{2\pi}\ln\left[\frac{\cot(8.13/2)}{\cot(30.35/2)}\right] \approx 80\Omega \tag{39}$$

The reflection coefficient when driven by a 50 Ω line will be

$$\Gamma = \frac{50-80}{50+80} = -0.231 , \tag{40}$$

with a resulting standing wave ratio of

$$SWR = \frac{1+|\Gamma|}{1-|\Gamma|} = \frac{1+0.231}{1-0.231} = 1.60 . \tag{41}$$

Instead of traveling all the way to the subreflector, however, the outer conductor of the conical transmission line will stop just before the point where it would intercept the ray that originates from the shadow zone boundary of the subreflector. Without a rigorous demonstration, it turns out that this length will be approximately 9.75 inches. At this point the end will turn back toward the main reflector and follow a path parallel with the inner most ray. The inner angle of the outer conductor will be approximately 70-degrees, and it will be fitted with a 1-inch radius at the point where it turns back to the main reflector. The outer conductor will stop such that it clears the surface of the main reflector by 1-inch when all petals of the main reflector are in the forward most position.

Note that the conical transmission line impedance of $Z_0 = 80\Omega$ is consistent with the peak gain system impedance of $Z_{System}^{Peak\ Gain} = 75\Omega$ and should result in a near optimum value of gain for the COBRA III prototype.

6. COBRA III SYSTEM DESIGN SUMMARY

In this section a brief summary of the design of the COBRA III prototype is presented. Common to the COBRA II and COBRA III prototype antennas are the main reflector and the subreflector. More detailed descriptions of these components can be obtained in [2].

6.1 Main Reflector

The main reflector is a paraboloidal surface with a usable diameter of 62.5 inches, and a focal length to diameter ratio of 0.25. It has been partitioned into 4 equal segments, with individual positioning capability and control.

6.2 Subreflector

The subreflector is a hyperboloidal surface with its convex side facing the main reflector, and with its prime focus located at the prime focus of the main paraboloidal reflector. Its conjugate focus is located at the vertex of the main reflector. Its axis is coincident with the axis of the main reflector, and its apex (the closest point on the subreflector) is 14 inches from the vertex of the main reflector. Its eccentricity is 1.623, which places the prime focus of the main reflector and the subreflector 2 inches behind the apex of the subreflector. The subreflector diameter is slightly oversized at 20.5 inches. The shadow region on the subreflector (the inner diameter of the subreflector for which rays are blocked by the subreflector as they reflect off the main reflector) is approximately 4 inches.

6.3 Conical Coaxial Transmission Line Feed

The conical coaxial transmission line will have a nominal characteristic impedance of $Z_0 = 80\ \Omega$ based on the half angles of the inner and outer conductors. The inner conductor will attach to the directly to the subreflector and have a nominal diameter of 4 inches at the attachment pont. The outer conductor will continue from the vertex, to a point along the conical path just before it intercepts the inner most ray path off of the subreflector. At this point the edge will be turned and radiused, and it will continue along a path parallel with the inner most ray path. It will not terminate on the main reflector, rather it will stop abruptly at a point where it will clear all of the moving surfaces of the main reflector.

A schematic rendering of the COBRA III prototype antenna in the $N = 4$ configuration is shown in Figure 6. The inner and outer conductors of the conical transmission line feed are visible, as well as the outer conductor collar. Also, a (styrofoam) structure is seen to support to center conductor of the conical transmission line.

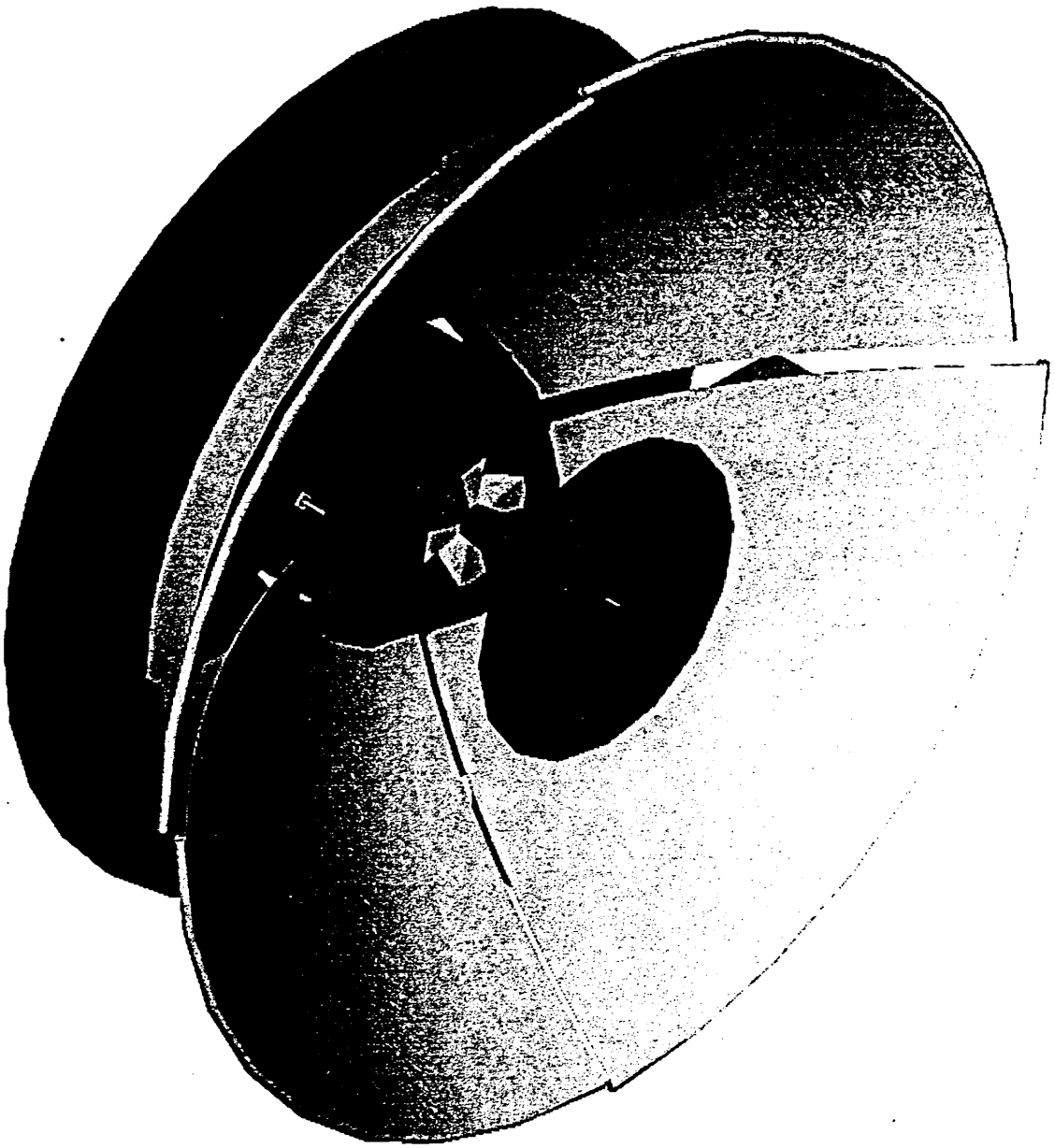

Figure 6. **A schematic rendering of the COBRA III prototype antenna in the $N = 4$ configuration is shown. The inner and outer conductors of the conical transmission line feed are visible, as well as the outer conductor collar.**

REFERENCES

1. "Coaxial Beam-Rotating Antenna (COBRA) Concepts," C. Courtney and C. Baum, Sensor and Simulation Note No. 395, April 1996.
2. "Design and Measurement of a Cassegrain-type Coaxial Beam-Rotating Antenna," C. Courtney et al, Sensor and Simulation Note No. 427, November 1998.
3. "Considerations for a GW-level COBRA Antenna Design," C. Courtney, et al, Eighth National Conference on High Power Microwave Technologies, Johns Hopkins University, April 8 – 10, 1997.
4. "Increasing the RF energy per Pulse of an RKO," K. Hendricks, et al, IEEE Trans. on Plasma Science, vol. 26, no. 3, June 1998.
5. "Concepts and Performance Estimates of the Coaxial Beam Rotating Antenna (COBRA)," C. Courtney, C. Baum, and R. Torres, Proceedings of the IEEE 1996 Symposium on Antennas and Propagation, Baltimore, MD.
6. Robert E. Collin, *Antennas and Radiowave Propagation*, McGraw-Hill, New York, 1985.
7. "Performance and pulse shortening effects in a 200-kV PASOTRON HPM source," D. Goebel, R. Schumacher and R. Eisenhart, IEEE Trans. on Plasma Science, vol. 26, no. 3, June 1998.
8. "Investigation of RF Breakdowns on the MILO," D. Schiffler, et al, IEEE Trans. on Plasma Science, vol. 26, no. 3, June 1998.
9. "Prepulse associated with the TEM feed of an impulse radiating antenna," E. Farr and C. E. Baum, Sensor and Simulation Note No. 337, March 1992.
10. Roger F. Harrington, *Time-Harmonic Electromagnetic Fields*, McGraw-Hill, New York, 1961.